

# High-spectral-resolution pulsed photoluminescence study of molecular-beam-epitaxy-grown GaAs/Al<sub>x</sub>Ga<sub>1-x</sub>As multi-quantum-well structures using a very-low-power tunable pulsed dye laser

M. Naganuma,<sup>a)</sup> J. J. Song, and Y. B. Kim

*Department of Physics, University of Southern California, Los Angeles, California 90089-0484*

W. T. Masselink and H. Morkoç

*Coordinated Science Laboratory, University of Illinois, Urbana, Illinois 61801*

T. Vreeland, Jr.

*California Institute of Technology, Pasadena, California 91125*

(Received 13 January 1986; accepted for publication 15 May 1986)

Ultralow-power, high-resolution, pulsed-laser photoluminescence (PL) and photoluminescence excitation (PLE) spectroscopies were carried out in molecular-beam-epitaxial GaAs/Al<sub>x</sub>Ga<sub>1-x</sub>As multi-quantum-well structures at 5 K. Fine structures were observed for the first time in the PLE spectra, both in the heavy-hole and light-hole excitonic regions. Most of the fine structures are considered to arise from monolayer fluctuations in the thicknesses of the GaAs wells. Dramatic changes in the line shapes and the peak positions of the PL and PLE spectra were observed by applying selective PL detection and excitation spectroscopic techniques.

## I. INTRODUCTION

Recent progress in molecular beam epitaxy (MBE) has produced highly sophisticated superlattice (SL) structures whose layer thickness can be controlled to the accuracy of an atomic monolayer.<sup>1</sup> The development of growth techniques has been accompanied by observation techniques on the atomic scale, such as transmission electron microscopy (TEM).<sup>2</sup> TEM, however, is a destructive method and its sample preparation is still in the state of the art. Nondestructive methods such as photoluminescence (PL) spectroscopy can also provide atomic-scale information about the layer thicknesses of superlattices.<sup>3-7</sup>

Previous photoluminescence studies in superlattices have been carried out mostly by using cw laser sources such as argon-ion or krypton-ion lasers.<sup>8-10</sup> For pulsed-laser-induced photoluminescence studies, most of the work was done at relatively high power levels with excitation laser photon energies significantly above the  $n = 1$  quantized states in superlattices.<sup>11</sup> Consequently, the PL spectra detected with pulsed lasers did not exhibit fine structures which can be used to extract the microscopic details of the heterostructure samples.

In this work, an ultralow-power pulsed-laser-induced photoluminescence study is reported with MBE-grown GaAs/Al<sub>x</sub>Ga<sub>1-x</sub>As superlattices at 5 K. Particular attention was paid to the fine structures in the excitonic heavy-hole region of the PL spectra. By making the excitation laser wavelength resonant with the light-hole energy of the SL, microwatt ( $\mu\text{W}$ ) peak power was sufficient to observe the PL spectra. In addition, dramatic changes in the fine structures of PL spectra have been observed when tuning the laser wavelength in the vicinity of the light-hole energy level of the

SL samples. The results are interpreted to arise in part from the layer-thickness fluctuations. The corresponding fine structures in the light-hole region are detected by PL excitation (PLE) spectroscopy by tuning the laser wavelength. To the best of our knowledge, this work is the first report on successful applications of very-low-power ( $\mu\text{W}$  range) pulsed lasers to PL and PLE spectroscopy, as well as on observations of fine structures in the light-hole region.

## II. EXPERIMENT

The superlattice samples GaAs/Al<sub>x</sub>Ga<sub>1-x</sub>As were grown by MBE on Si-doped GaAs(100) substrates at 600 °C. Details on the MBE sample growth is described in Ref. 12. Both the well and the barrier layers were undoped. Sample parameters such as the well width  $L_z$ , the barrier width  $L_b$ , and the AlAs mole fraction in the barrier layer  $x$  were determined by x-ray double-crystal diffraction with data-fitting analyses combined with the MBE growth conditions.<sup>13</sup> Symmetric (400) and (200) rocking curves were analyzed to obtain  $L_z$  and  $L_b$  (from the angular separation of superlattice peaks) and the average Al content in the superlattice (from the position of the zero-order superlattice peak with respect to the substrate peak). The ratio of  $L_z$  to  $L_b$  was found by matching observed and calculated amplitudes of the superlattice peaks, with the aluminum fraction  $x$  calculated from the average Al content,  $L_z$  and  $L_b$ .

The photoluminescence excitation source was a tunable dye laser pumped by a pulsed Nd:YAG laser (YAG denotes yttrium aluminum garnet). The pulse duration, the repetition rate and the laser linewidth were 7 nsec, 10 Hz, and 0.025 meV [full width at half maximum (FWHM)], respectively. One of the advantages of using a pulsed Nd:YAG laser-pumped dye laser system is the wide wavelength range it can cover. The PL signal was detected from SL samples at low temperatures by a cooled photomultiplier in conjunc-

<sup>a)</sup> Permanent address: Electrical Communications Laboratory, Nippon Telegraph and Telephone Corp., Musashino, Japan.

tion with a double monochromator and a gated boxcar integrator. The boxcar, the spectrometer, and the dye-laser tuning system were interfaced to a computer for automatic data acquisition. For off-resonant photoluminescence studies, LDS698 dye solution was used, whereas for resonant PL studies, LDS698 dye solution was found to be very convenient to use, since its output power level is nearly constant in the excitonic regions of the SL samples reported here. The typical scanning rate of the dye laser used in this work was  $0.5 \text{ \AA/s}$ .

The dye-laser output beam was filtered through a diaphragm of 1 mm diameter and loosely focused by a lens of focal length 30 cm. The laser-beam spot size on the sample was estimated to be  $500 \mu\text{m}$  in diameter. The excitation power could be varied over a very wide range with neutral-density filters. The PL signal could be detected over 10 orders of dynamic range in excitation power. The excitation energy density down to  $1.3 \times 10^{-11} \text{ J/pulse cm}^2$  was sufficient for the PL signal detection.

Different areas on the samples could be investigated without disturbing the optical alignment since the liquid-helium cryostat was conveniently mounted on xyz translation stages.<sup>14</sup> This capability was important to check possible spot-to-spot variation in MBE sample structures. No significant variations were detected within the sample surface area of  $\sim 2 \times 2 \text{ mm}^2$ .

### III. RESULTS AND DISCUSSION

At low excitation power levels of the pulsed-laser beam, the photoluminescence signals arise from the  $n = 1$  heavy-hole excitonic region. With an increase of the laser power level, however, the PL from the excited energy levels (i.e.,  $n > 1$ ) is detected even at low temperatures. This is in contrast to the case of cw PL spectroscopy, in which PL from the excited states is detected in most cases, only at elevated temperatures.<sup>15</sup>

Figure 1 depicts the spectra taken from a superlattice sample at 5 K at two different laser power levels. The sample has a well size ( $L_z$ ) of  $95 \text{ \AA}$  and the AlAs mole fraction in the barrier layer ( $x$  value) of 24%. The number of periods and the barrier thickness ( $L_b$ ) are 40 and  $95 \text{ \AA}$ , respectively. The low-power spectrum [Fig. 1(b)] is observed in the energy region of  $1.550 \text{ eV}$ . The spectrum (b) is associated with optical transitions of excitons involving  $n = 1$  electrons to the heavy-hole transitions. At high excitation levels, new peaks are revealed as depicted in spectrum (a) at both the higher- and lower-energy sides of the spectrum (b), in the regions of  $1.64$  and  $1.49 \text{ eV}$ , respectively. These peaks begin to emerge at carrier densities of about  $10^{15}/\text{cm}^3$ . Both the spectra (a) and (b) were taken at an excitation laser wavelength  $7000 \text{ \AA}$  ( $1.8 \text{ eV}$ ) using a LDS698 dye solution.

In spectrum (a), the peak on the higher-energy side is attributed to transitions from the  $n = 2$  quantized electron states to the heavy-hole level associated with the band-filling effect.<sup>16</sup> The lower-energy peak at  $\sim 1.5 \text{ eV}$  originates in part from the substrate material. The PL signals from the substrate would be reabsorbed by the GaAs buffer layer (between the substrate and the superlattice) when the reflection (backscattering) geometry is employed as in this work.

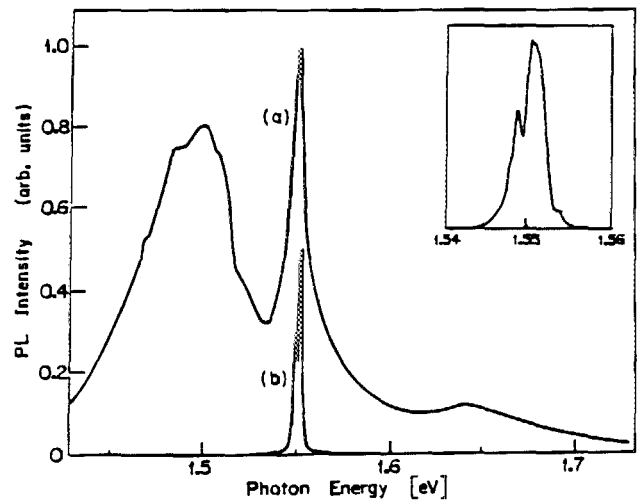


FIG. 1. Two photoluminescence spectra taken from a GaAs/ $\text{Al}_x\text{Ga}_{1-x}\text{As}$  multi-quantum-well structure using a pulsed dye laser of wavelength  $7000 \text{ \AA}$  at two different laser-power levels. The laser peak power level used for (b) is about 9 orders of magnitude less than that for (a). The photoluminescence peak intensities of spectra (a) and (b) were arbitrarily adjusted to show clearly the difference in spectral shapes. The inset shows spectrum (a) in a magnified horizontal scale.

This reabsorption would then appear as a dip in the PL spectra. The sharp drop of the PL signals and a small dip at  $1.52 \text{ eV}$  is explained as manifestations of GaAs exciton reabsorption in the buffer layer of the sample.<sup>17</sup> Although not shown here, the dip is more obvious in the spectra taken at somewhat lower excitation levels than that used for the spectrum (a).

The low-power spectrum (b) is magnified in the inset. Splittings and substructures are clearly shown. As the excitation power was increased, the splitting became blurred with the increase of the half-width of each peak. Eventually, at higher excitation power levels, only a single peak was observed in the spectrum. This fact indicates that in the previously reported pulsed-laser PL spectroscopy work, a set of peaks could have been observed as a single peak due to the

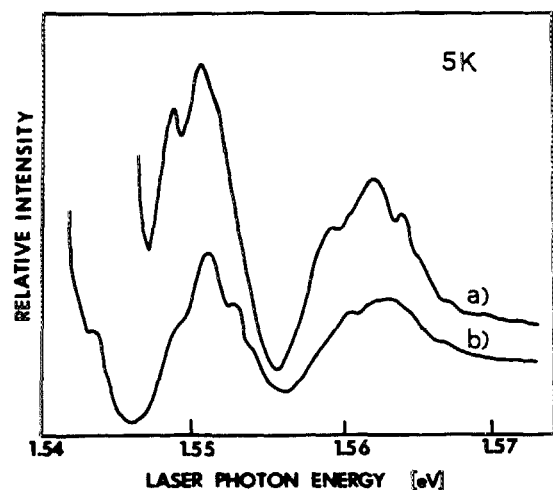


FIG. 2. High-resolution photoluminescence excitation spectra exhibiting fine structures. Spectra were taken from the same sample as shown in Fig. 1 with a low-power pulsed dye laser. The detection energy positions of (a) and (b) are  $1.544$  and  $1.539 \text{ eV}$ , respectively.

higher power level used than in our case.

Figure 2 shows PL excitation spectra taken with the same sample as in Fig. 1. In PL excitation spectroscopy, the PL detection energy is fixed (in this work, by the spectrometer setting), while the laser wavelength is tuned. The two spectra in Fig. 2 were taken at two different PL detection energies, 1.5436 and at 1.5367 eV for the curves (a) and (b), respectively. PLE spectral shapes are found to be dependent upon detection energies. It is also noticed that the half-width of the PL excitation spectrum for the light-hole exciton is larger than that for the heavy-hole exciton, and therefore, it is more difficult to resolve the fine structures in the vicinity of the light hole.

For the simultaneous observation of both the heavy-hole and the light-hole PL excitation spectra as exhibited in Fig. 2 the detection energy was set in the tail of the heavy-hole excitonic peaks, sufficiently away from the major features of the spectrum. This is the case for Fig. 2 in this work as well as for most of the previously reported PLE spectra.<sup>18</sup> Resonant PL excitation spectroscopy which will be discussed below can yield additional information on SL samples which cannot be extracted by ordinary PLE spectroscopy work as demonstrated below. In resonant PL excitation spectroscopy the detection energy is set to coincide with a particular peak energy of the PL spectra where the signal levels are high. In this case, the detection energy bandwidth (the spectrometer slit width) can be kept narrow so that PL signals from the adjacent peaks cannot pass through the detector system. Then the excitation energy is varied (laser wavelength tuning) across certain excited states of the superlattice sample. This technique can compliment the resonant photoluminescence technique, where the laser excitation energy is set to coincide with a particular energy level of the sample while the PL spectra are obtained by varying the detector frequency (spectrometer tuning). We have applied both of these resonant PL and resonant PL excitation spectroscopy methods to the superlattice samples, and observed, for the first time to our knowledge, substructures both in the heavy-hole and light-hole excitonic regions.

By employing selective PL and PLE spectroscopy techniques, more than four discrete substructures were found in both the heavy- and the light-hole regions of the GaAs/Al<sub>x</sub>Ga<sub>1-x</sub>As ( $x \sim 0.165$ ) sample with 40 periods of  $L_z \sim 92 \text{ \AA}$  and  $L_b \sim 95 \text{ \AA}$ . Figure 3(a) depicts the PL spectra taken with different excitation energies. Curves (a), (b), (c), and (d) were obtained with excitation photon energies at 1.5573, 1.5591, 1.5609, and 1.5632 eV, respectively. These excitation energies correspond to the peak energies of the light-hole PLE spectra (see Fig. 4). When slightly different excitation energies were employed than those used in Fig. 3(a), these four substructures still remained as dominant features, indicating that these peaks represent main channels of radiative recombination of excited carriers. Considering the fact that dramatic changes in PL spectra are observed with only a couple of meV changes in excitation photon energies, it is obvious that the linewidth of the laser used in the experiments should be narrow (compared to the PL peak width), and the laser-beam quality, good in terms of its spectral purity, for the observation of these fine structures. Also,

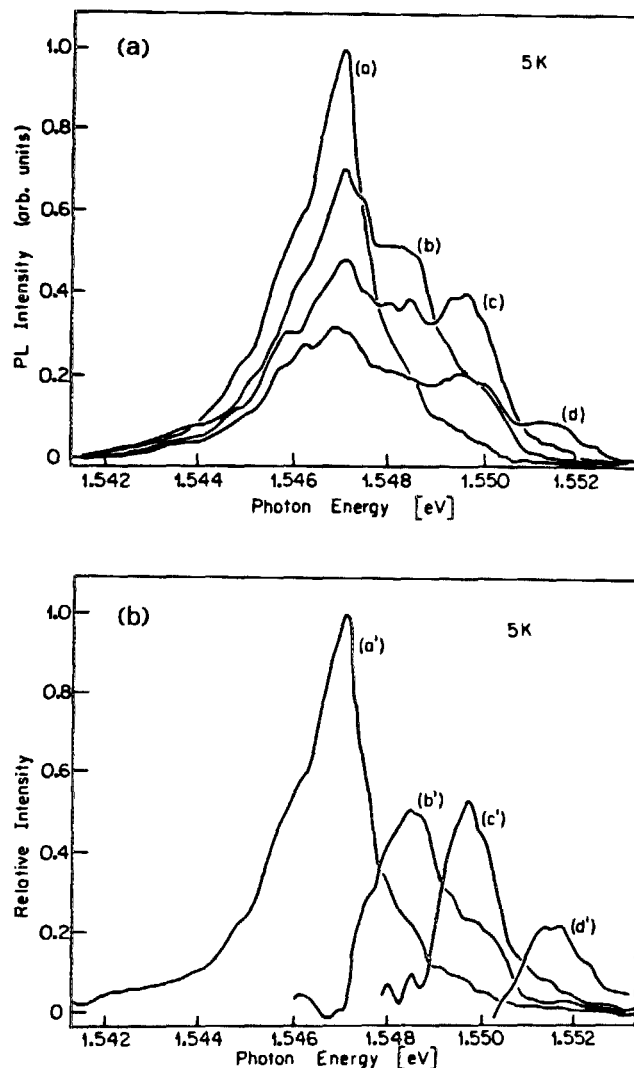


FIG. 3. (a) Resonant photoluminescence spectra in the heavy-hole exciton region of a GaAs/Al<sub>x</sub>Ga<sub>1-x</sub>As multi-quantum-well structure. Drastic changes in the PL spectra are detected when the excitation laser wavelengths are fine tuned in the light-hole exciton region. The excitation laser photon energies for the spectra (a), (b), (c), and (d) are 1.5570, 1.5587, 1.5605, and 1.5632 eV, respectively. (b) Spectra in part (a) are shown to be a combination of peaks whose energetic positions are distinctly separated from one another. See text for details.

these variations in spectral shapes can not be observed without a high-resolution detection system. For example, if a detection bandwidth of  $\sim 4 \text{ meV}$  (FWHM) had been employed, the spectra (b) and (c) might have appeared as one single peak. This observation confirms the usefulness of the high-resolution PL spectroscopy in SL characterizations. What is noteworthy in Fig. 3(a) is that the spectrum becomes broader and more structures appear as the excitation photon energy is increased. The sharpness of the peak is also noteworthy, indicating the high quality of the superlattice sample examined here. The broader spectra are also considered to be the superpositions of several narrow peaks, the half-width of which are approximately same as that of the peak (a). This aspect is more clearly depicted in Fig. 3(b).

In Fig. 3(b), four discrete spectra are presented. The spectrum (b') was deduced from the spectrum (b) in Fig. 3(a) by subtracting (a) from (b). Similarly (c') and (d')

were derived by subtracting (b) from (c), and (c) from (d), respectively. Note that the spectra were normalized to the same signal level of the lowest peak at 1.547 eV before subtraction for the purpose of comparing the spectral shapes. From Fig. 3(b), it can be said that (b) is in fact a superposition of two peaks (a') and (b'), and that the broad spectrum (d) consists of four discrete peaks (a'), (b'), (c'), and (d'). It is interesting to note that separations of the peaks in Fig. 3(b) are same. The peaks (a'), (b'), and (c') are equidistant on the energy scale, whereas the energy separation between (c') and (d') is slightly larger. From this observation and its low signal level, it appears that the origin of the peak (d') is different from that of the rest. One possible explanation is that (d') represents free-exciton transitions and (a'), (b'), and (c') come from donor-bound-exciton transitions.<sup>19</sup> It is also our conjecture that there are additional small peaks similar to (d') in their origins which are buried under the stronger and narrower peaks (a'), (b'), and (c').

In PL spectra shown in Fig. 3(a), as the excitation photon energy is increased, the corresponding higher-side-energy peak is resonantly enhanced as expected. The lower-energy portion of the spectra, however, does not disappear completely. This is because the lower-energy peaks can still be excited off-resonantly via the continuum states. It is also noticed that the radiative recombination channel represented by peak (a) seems to have high PL efficiency. Otherwise, the spectra (b), for example, could have appeared nearly as a single peak centered at 1.5484 eV, resembling (b') with a tail in the lower-energy side, rather than as a double-peaked feature as observed here. Also, the integrated PL intensities of the four spectra (area under the curve) shown in Fig. 3(a) are approximately same for the same number of excitation photon densities.

What has been discussed with Figs. 3(a) and 3(b) concerns with energy substructures revealed in the PL emission

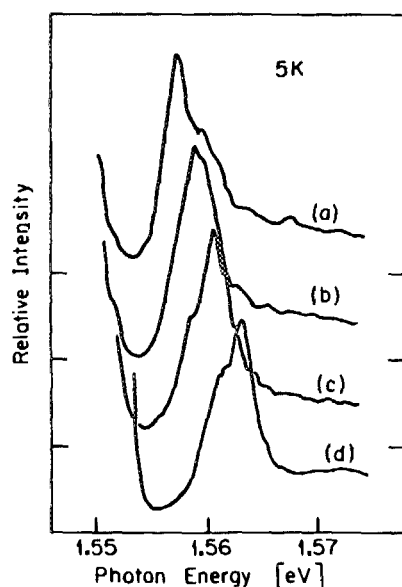


FIG. 4. Light-hole exciton region PL excitation spectra. The PL detection energies of spectra (a)–(d) correspond to peak energy positions of (a')–(d') in the PL spectra shown in Fig. 3. The spectra are translated vertically for easy comparison.

spectra detected at low temperatures in the heavy-hole excitonic region of the SL. Information on energy substructures in the light-hole region was deduced by performing PL excitation spectroscopy in the following manner. The PL detection system was set in such a way that signals from only one peak, say peak (a), in the heavy-hole region could be collected. Then, the pulsed-dye-laser wavelength was scanned through the light-hole excitonic region.

Figure 4 shows four PL excitation spectra taken with the detector bandwidth centered at four different peak positions in Fig. 3, namely, 1.5470, 1.5484, 1.5498, and 1.5514 eV. When varying the detection energy, the peak position of the PLE spectrum is shifted. It is noticed that for each heavy-hole peak, there is a corresponding light-hole associated peak. By observing the slope of the rise and fall of each spectrum, the light-hole exciton related discrete energy states appear to be pretty well contained between (a) and (d). No significant light-hole related excitonic states, are thought to occur below (a) and above (d) considering the asymmetric shapes and the abruptness of the slope at the rising and the falling edges of (a) and (b), respectively.

The experimentally observed peaks separated by  $\sim 1.4$  meV in the heavy-hole region (see Fig. 3) can be taken as manifestations of monolayer (2.82 Å) fluctuations in the well sizes. The splittings observed are in reasonable agreement with calculated values of  $\sim 1.6$  meV considering the uncertainties involved in sample parameters. The calculations were carried out by using the effective-mass approximation and sample parameters as follows<sup>20</sup>: the energy-gap difference  $E_g(\text{Al}_x\text{Ga}_{1-x}\text{As}) - E_g(\text{GaAs}) = 1.247x$  eV, the conduction-band to the valence-band split-off ratio  $\Delta V_c/\Delta V_v = 60/40 - 65/35$ , and effective masses  $m_e/m_0 = 0.067$ ,  $m_{hh}/m_0 = 0.35$  for GaAs and  $m_e/m_0 = 0.081$ ,  $m_{hh}/m_0 = 0.358$  for  $\text{Al}_x\text{Ga}_{1-x}\text{As}$  ( $x \sim 0.165$ ). One interesting observation is that the energy splitting in the light-hole exciton transitions are approximately 25% larger than those in the heavy-hole exciton transitions as predicted by calculations using the aforementioned sample parameters in conjunction with  $m_{lh}/m_0 = 0.094$  and 0.105 for GaAs and  $\text{Al}_x\text{Ga}_{1-x}\text{As}$  ( $x \sim 0.165$ ), respectively. If we assume  $\Delta V_c/\Delta V_v = 85/15$ , energy-level splittings due to the monolayer fluctuations in the light-hole region are calculated to be almost same as those in the heavy-hole region. This certainly is not the case in our experimental data.

The observation of several peaks equally spaced on the energy scale both on the heavy- and the light-hole regions were explained as an indication that the GaAs well sizes inside the superlattice sample are not uniform but differ by one monolayer thickness 2.82 Å. There can, however, be well-size inhomogeneities within a layer (intralayer inhomogeneity) and/or among different layers (interlayer inhomogeneity).

In general, MBE-grown superlattice interfaces are not planar but considered to consist of islands with steps of monolayer thickness. The island sizes are thought to be reflected in the spectral width of the photoluminescence from superlattice samples. The PL linewidth of the sample shown in Fig. 3 is estimated to be  $< 1.2$  meV (FWHM). According to the calculations of Singh and co-workers, this linewidth

leads to the estimations of island size (diameter) of  $< 80 \text{ \AA}$  which is much smaller than the exciton diameter ( $\sim 250 \text{ \AA}$ ).<sup>3,5</sup> This result rules out the possibility that the island intralayer fluctuations are dominantly responsible for the observed spectral substructures, except for cases where long-range (compared to exciton sizes) fluctuations are superimposed on the fluctuations mentioned above.

One can also consider layer-to-layer thickness fluctuations as one source of contributions to equidistant peaks. This picture is qualitatively supported in part by our preliminary PL experiments carried out at two different photon energies of 2 and 1.5 eV. The overall PL spectra are broader for the longer-wavelength excitation case than the shorter-wavelength case. We consider this an indication of spatial inhomogeneity along the MBE growth, i.e., the existence of layer-to-layer nonuniformity. The penetration depth into the sample of the excitation light is larger for longer wavelength, and consequently, more sample layers can be probed with 1.5-eV photons than with 2-eV photons.<sup>21</sup>

An additional source of the sample inhomogeneity may come from the unavoidable misorientation of the substrate material from the strict  $[100]$  direction. This misorientation can also cause intralayer nonuniformities in a different manner than the case of islandlike features. These irregularities, however, are believed to be more concentrated near the substrate material and presumably do not have significant effects on the very-low-power resonant PL spectra. Because of the larger number of wells inside the sample we studied, conclusive pictures of the layer inhomogeneity are not easy to derive. With a SL sample of a few layers, however, it is feasible to assign the origin of a certain peak to a particular layer. If the resonant PL and PLE spectroscopy work is performed with this peak, it essentially means that a certain layer of the SL samples is selectively studied. This capability of layer-by-layer selective characterization is unique to resonant PL and PLE techniques and not accessible by the conventional off-resonant PL spectroscopy work.

#### IV. SUMMARY

A very-low-power, high-resolution pulsed dye laser was used for the first time to study photoluminescence from MBE-grown  $\text{GaAs}/\text{Al}_x\text{Ga}_{1-x}\text{As}$  multi-quantum-well structures at 5 K. Fine structures were detected both in the heavy-hole and in the light-hole excitonic transition spectra. By employing selective detection and/or excitation spectroscopic techniques, multiplexes (fine structures) in the PL and PLE spectra could be separated. Furthermore, a weak optical transition state buried in the tail of a strong peak nearby can be clearly revealed. Fine structures which exhibit equidistant peaks are thought to arise from monolayer fluctuations in the well sizes. This is supported by calculations based on the effective-mass approximation.<sup>20</sup> It was also pointed out that the energy-level separations in the light-hole region are larger than those in the heavy-hole region in the samples we investigated.

The work reported here deals with  $n = 1$  quantum state of  $\text{GaAs}/\text{Al}_x\text{Ga}_{1-x}\text{As}$  but can easily be extended to higher energy optical transitions involving  $n > 1$ . Also, pulsed PL

spectroscopy will be very useful in studying samples such as  $\text{GaAs}/\text{In}_x\text{Ga}_{1-x}\text{As}$ , the energy gap of which is hard to reach by common cw dye lasers.

#### ACKNOWLEDGMENTS

We would like to acknowledge helpful discussions with Dr. D. C. Reynolds and Dr. J. Singh. One of us (M. N.) expresses his thanks to Dr. P. M. Petroff for illuminating discussions on MBE heterostructure interfaces. A critical reading of the manuscript by Dr. A. Fedotowsky is also appreciated. This work was supported by the Office of Naval Research and Air Force Office of Scientific Research.

<sup>1</sup>Molecular Beam Epitaxy and Heterostructures, edited by L. L. Chang and K. Ploog (Martinus Nijhoff, Netherlands, 1985); for a comprehensive bibliography up to 1983, see, for example, *Molecular Beam Epitaxy of III-V Compounds*, edited by K. Ploog and K. Graf (Springer, New York, 1984).

<sup>2</sup>P. M. Petroff, R. C. Miller, A. C. Gossard, and W. Wiegmann, *Appl. Phys. Lett.* **44**, 217 (1984); H. Okamoto, M. Seki, and Y. Horikoshi, *Jpn. J. Appl. Phys.* **22**, L367 (1983).

<sup>3</sup>J. Singh, K. K. Bajaj, and S. Chaudhuri, *Appl. Phys. Lett.* **44**, 805 (1984).

<sup>4</sup>C. Weisbuch, R. Dingle, A. C. Gossard, and W. Wiegmann, *Solid State Commun.* **38**, 709 (1981).

<sup>5</sup>D. C. Reynolds, K. K. Bajaj, C. W. Litton, P. W. Yu, J. Singh, W. T. Masselink, R. Fisher, and H. Morkoc, *Appl. Phys. Lett.* **46**, 51 (1985).

<sup>6</sup>L. Goldstein, Y. Horikoshi, S. Tarucha, and H. Okamoto, *Jpn. J. Appl. Phys.* **22**, 1489 (1983).

<sup>7</sup>B. Deveaud, J. Y. Emery, A. Chomette, B. Lambert, and M. Baudet, *Superlatt. Microstruct.* **1**, 209 (1985).

<sup>8</sup>H. Jung, A. Fisher, and K. Ploog, *Appl. Phys. A* **33**, 9 (1984); *Appl. Phys. A* **33**, 97 (1984), and references therein.

<sup>9</sup>V. Swaminathan, P. J. Anthony, J. R. Pawlik, and W. T. Tsang, *J. Appl. Phys.* **54**, 2623 (1983).

<sup>10</sup>E. E. Mendez, G. Bastard, L. L. Chang, L. Esaki, H. Morkoc, and R. Fisher, *Phys. Rev. B* **26**, 7101 (1982).

<sup>11</sup>See for example, A. Y. Xu, V. G. Kreismanis, and C. L. Tang, *Appl. Phys. Lett.* **44**, 136 (1984), and references therein.

<sup>12</sup>Ya Li Sun, W. T. Masselink, R. Fisher, M. V. Klein, H. Morkoc, and K. Bajaj, *J. Appl. Phys.* **55**, 3554 (1984).

<sup>13</sup>V. S. Speriosu and T. Vreeland, Jr., *J. Appl. Phys.* **56**, 1591 (1984).

<sup>14</sup>J. J. Song, and W. C. Wang, *J. Appl. Phys.* **55**, 660 (1984).

<sup>15</sup>P. W. Yu, C. Chandhuri, D. C. Reynolds, K. K. Bajaj, C. W. Litton, W. T. Masselink, R. Fisher, and H. Morkoc, *Solid State Commun.* **54**, 159 (1985).

<sup>16</sup>See for example, D. Fekete, S. Borenstain, A. Ron, E. Cohen, and R. D. Burnham, *Superlatt. Microstruct.* **1**, 245 (1985).

<sup>17</sup>M. Naganuma, J. J. Song, Y. B. Kim, W. T. Masselink, H. Morkoc, and D. C. Reynolds, *Bull. Am. Phys. Soc.* **30**, 1143 (1985).

<sup>18</sup>See for example, M. H. Meynadier, C. Delalande, G. Bastard, M. Voos, F. Alexandre, and J. L. Lievin, *Phys. Rev. B* **31**, 5539 (1985).

<sup>19</sup>D. C. Reynolds, private communication.

<sup>20</sup>For details, see W. T. Masselink, P. J. Pearah, J. Klem, C. K. Peng, H. Morkoc, G. D. Sanders, and Y. C. Chang, *Phys. Rev. B* **32**, 8027 (1985).

<sup>21</sup>J. J. Song, Y. S. Yoon, Y. B. Kim, M. Naganuma, W. T. Masselink, and H. Morkoc, *SPIE Proc.* **623** (to be published).